Electronic Supplementary Material (ESI) for New Journal of Chemistry.

Electronic Supplementary Information for:

Preparation of Amino-Substituted Anthraquinone: Study of the Intersystem Crossing and Application as Efficient Photoinitiators for Photopolymerization

Ruilei Wang,[a] Huaiman Cao,[a] Jianzhang Zhao[a]* and Fabiao Yu [b]*

[a] State Key Laboratory of Fine Chemicals, Frontier Science Center for Smart Materials, School of Chemical Engineering, Dalian University of Technology, 2 Ling Gong Road, Dalian 116024, P. R. China. *E-mail: zhaojzh@dlut.edu.cn (J.Z.)

[b] Key Laboratory of Hainan Trauma and Disaster Rescue, The First Affiliated Hospital of Hainan Medical University, Hainan Medical University, Haikou 571199, P. R. China *E-mail: yufabiao@hainmc.edu.cn (F. Y.)

Contents

1. NMR and HRMS Spectra

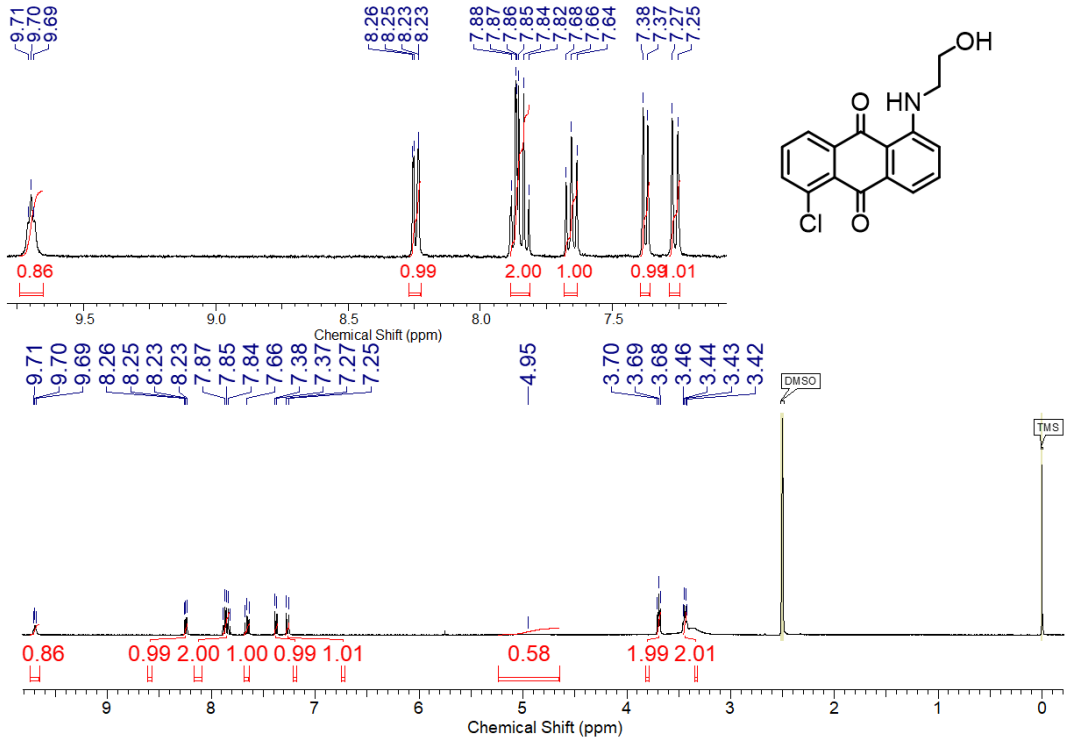

Figure S1. ^{1}H NMR spectrum of compound **AQ-NH-OH-5-Cl** (DMSO-d_6, 400 MHz).

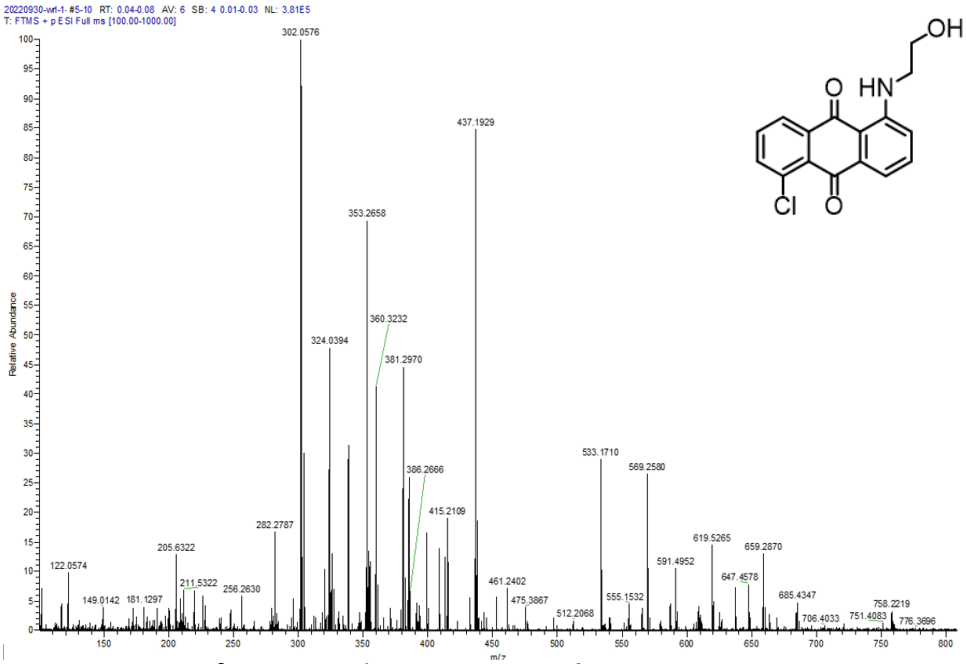

Figure S2. HRMS ESI^{+} of compound **AQ-NH-OH-5-Cl**.

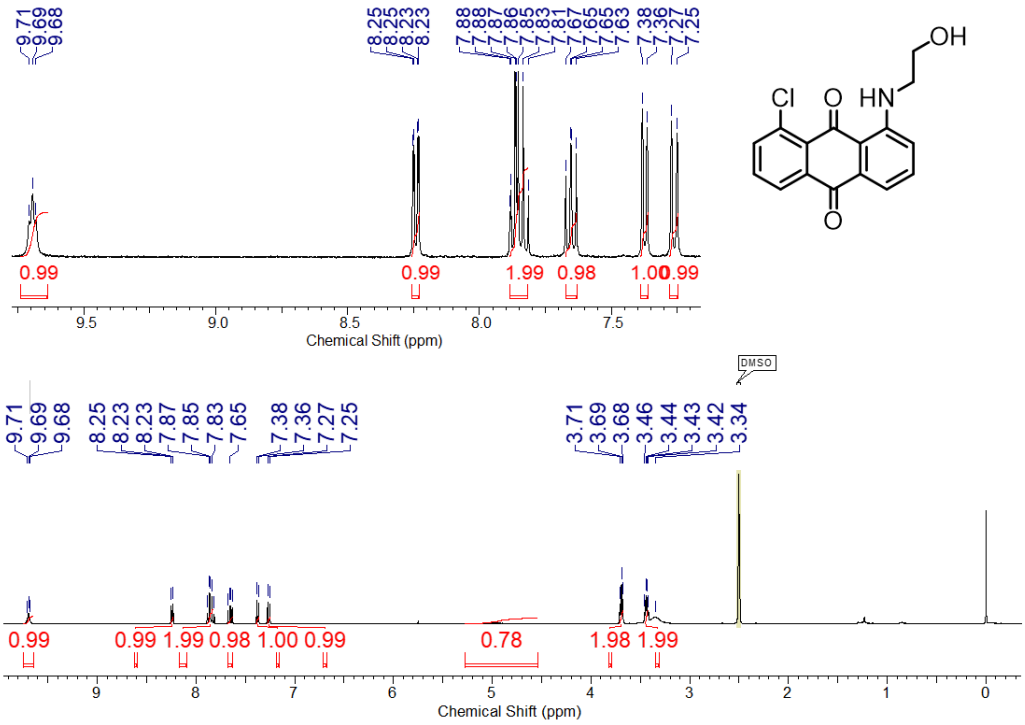

Figure S3. ^{1}H NMR spectrum of compound **AQ-NH-OH-8-Cl** (DMSO-d_6, 400 MHz).

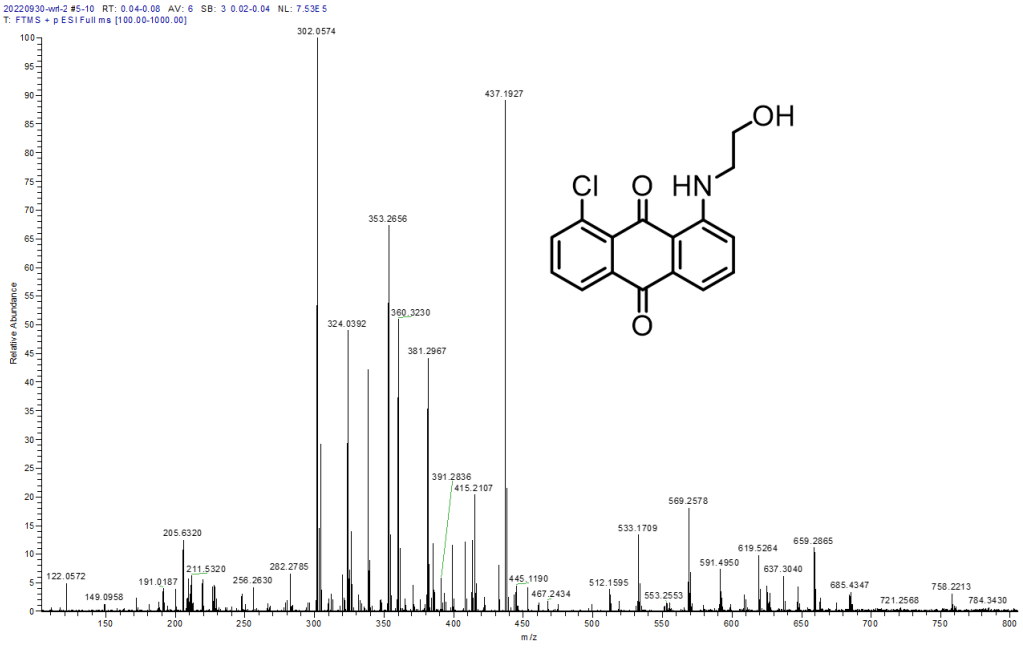

Figure S4. HRMS ESI^{+} of compound **AQ-NH-OH-8-Cl**.

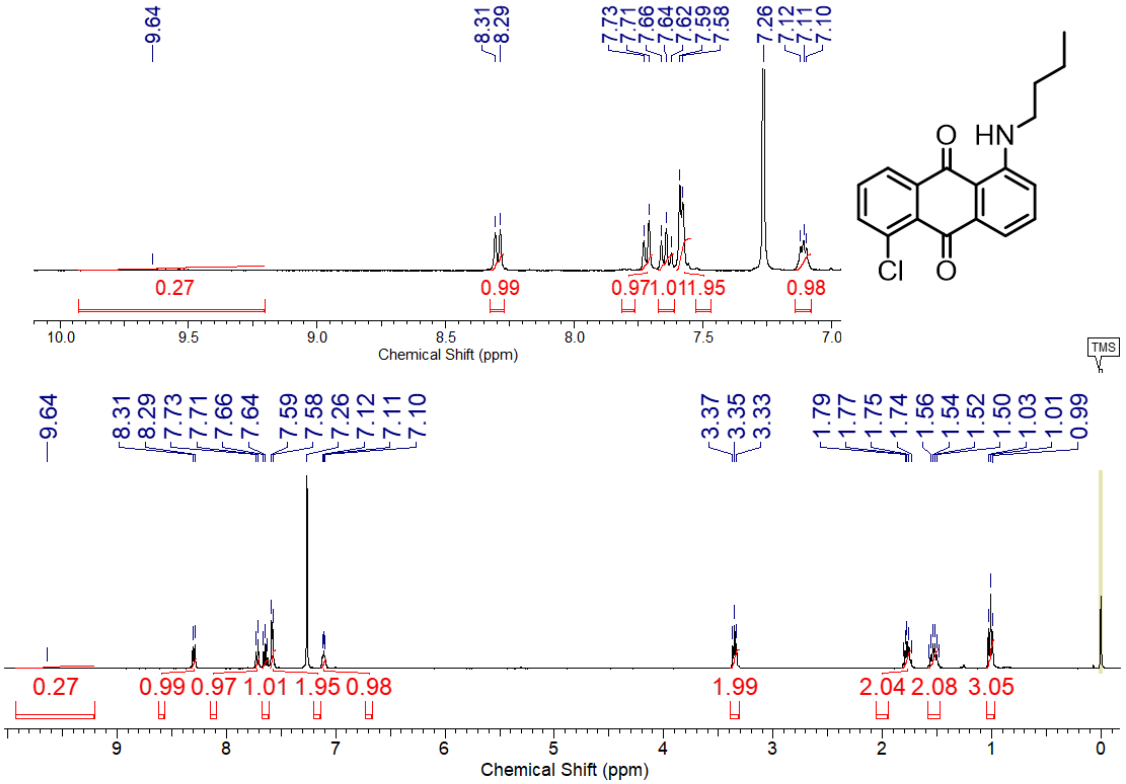

Figure S5. ^{1}H NMR spectrum of compound **AQ-NH-5-Cl** ($CDCl_3$, 400 MHz).

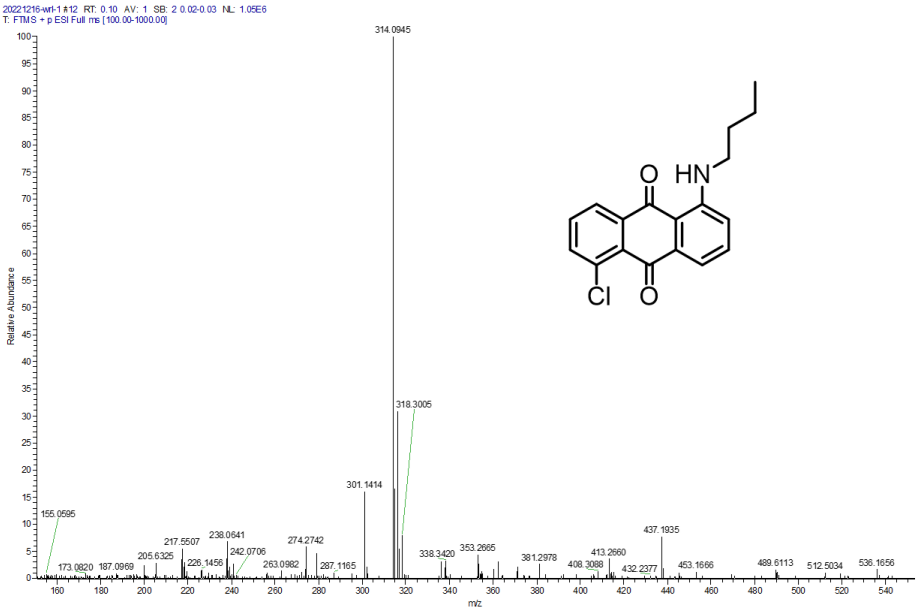

Figure S6. HRMS ESI^{+} of compound **AQ-NH-5-Cl**.

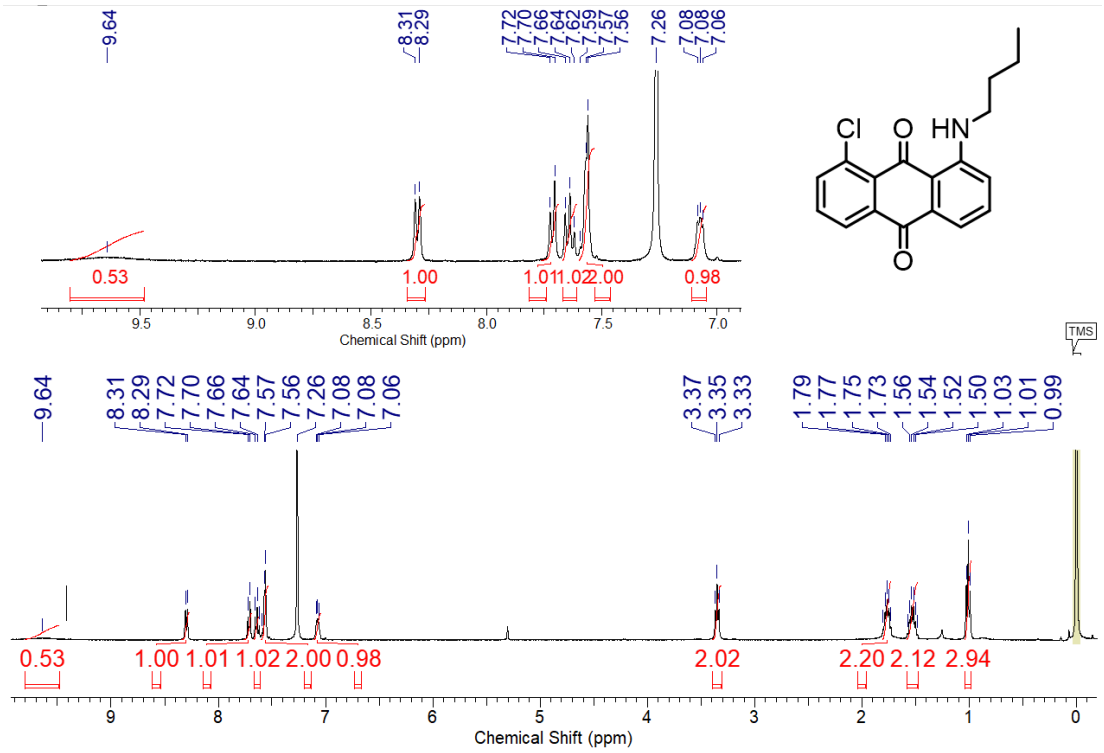

Figure S7. ^{1}H NMR spectrum of compound **AQ-NH-8-Cl** ($CDCl_3$, 400 MHz).

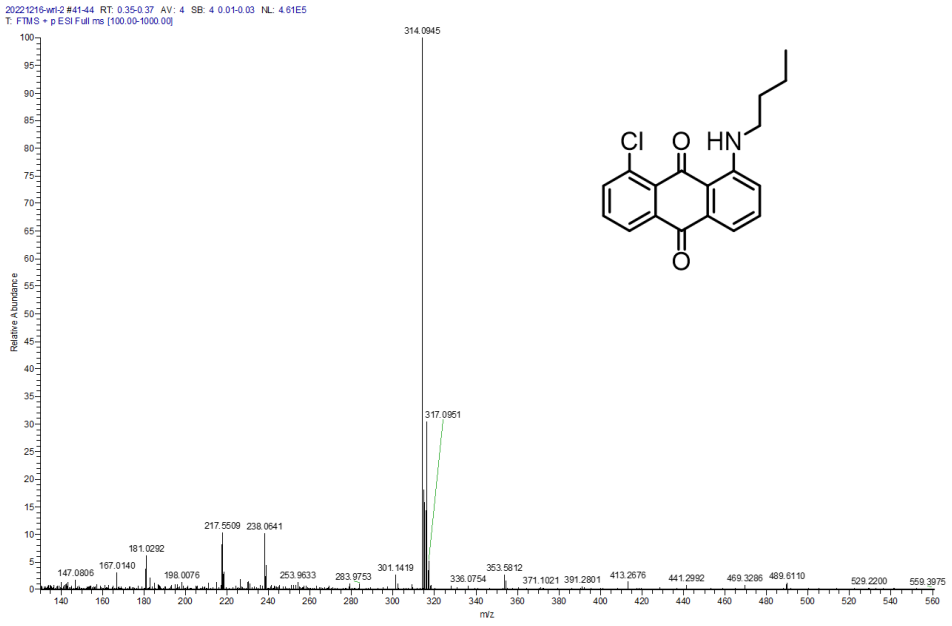

Figure S8. HRMS ESI^{+} of compound **AQ-NH-8-Cl**.

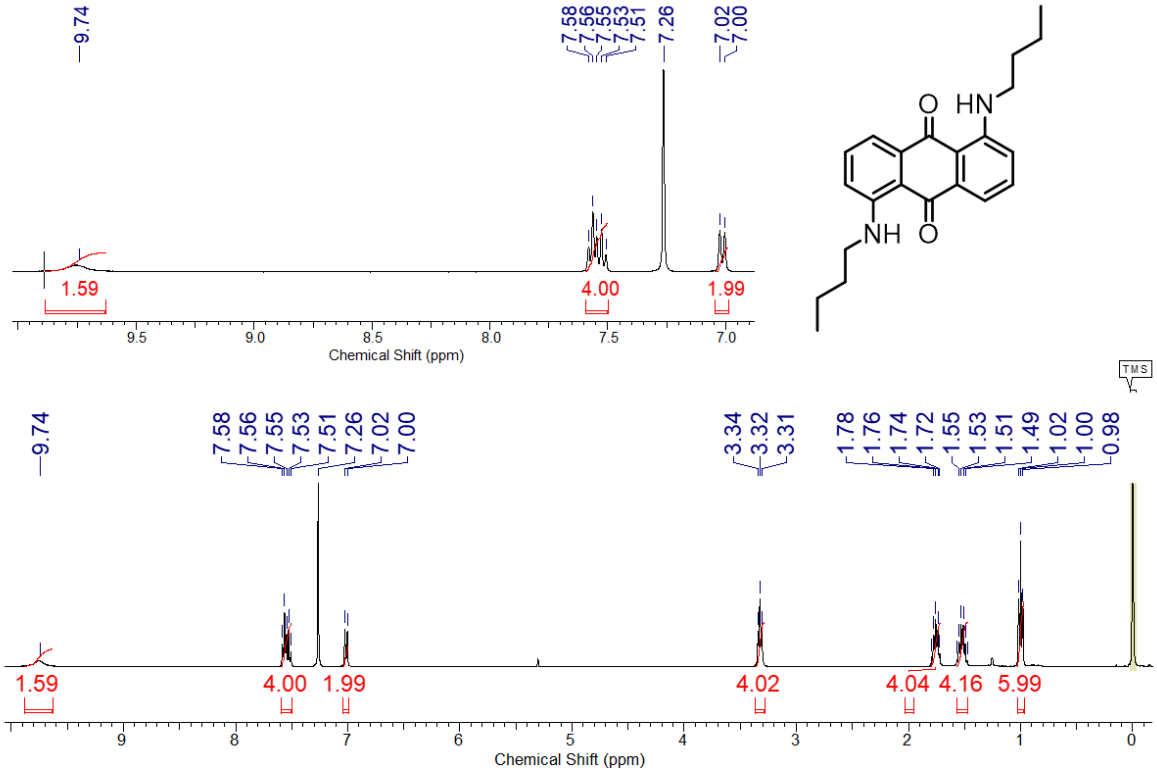

Figure S9. ^{1}H NMR spectrum of compound **AQ-1,5-NH** ($CDCl_3$, 400 MHz).

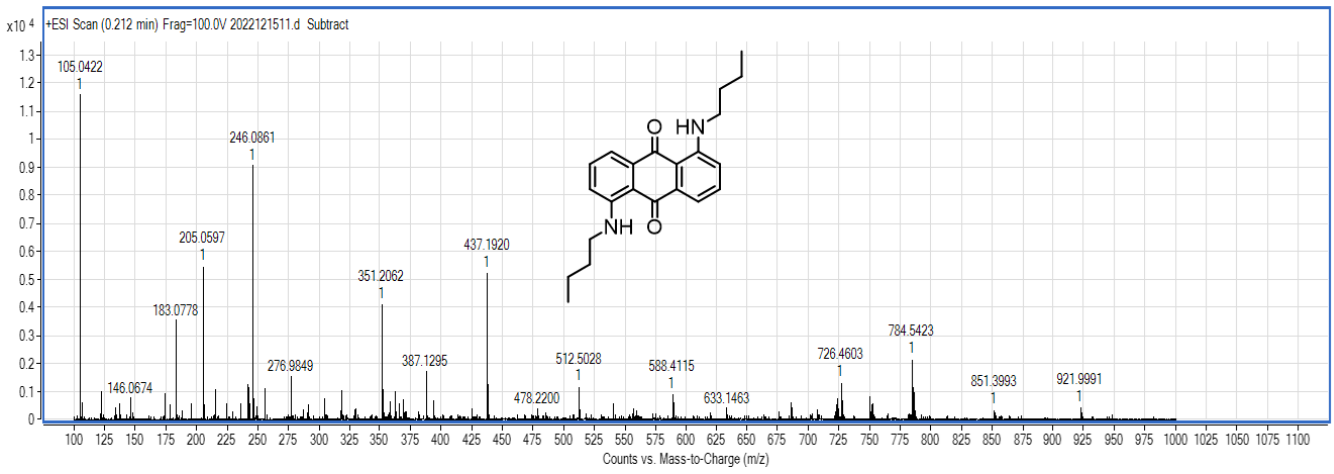

Figure S10. HRMS ESI^{+} of compound **AQ-1,5-NH**.

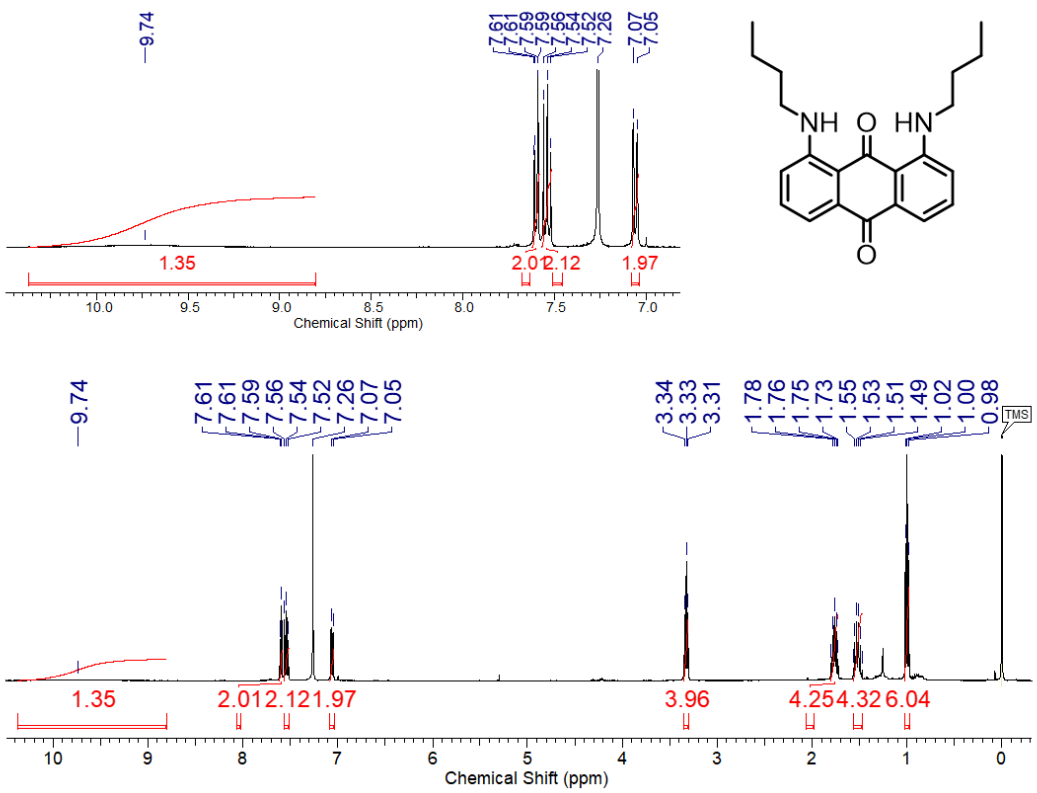

Figure S11. ^{1}H NMR spectrum of compound **AQ-1,8-NH** ($CDCl_3$, 400 MHz).

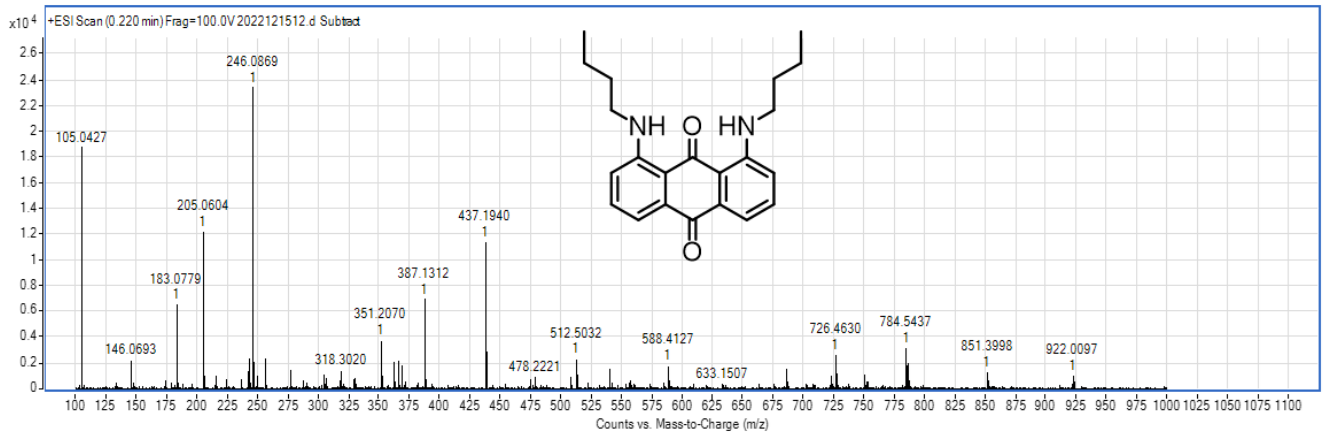

Figure S12. HRMS ESI^{+} of compound **AQ-1,5-NH**.

2. Steady State UV–Vis Absorption and Luminescence Spectra

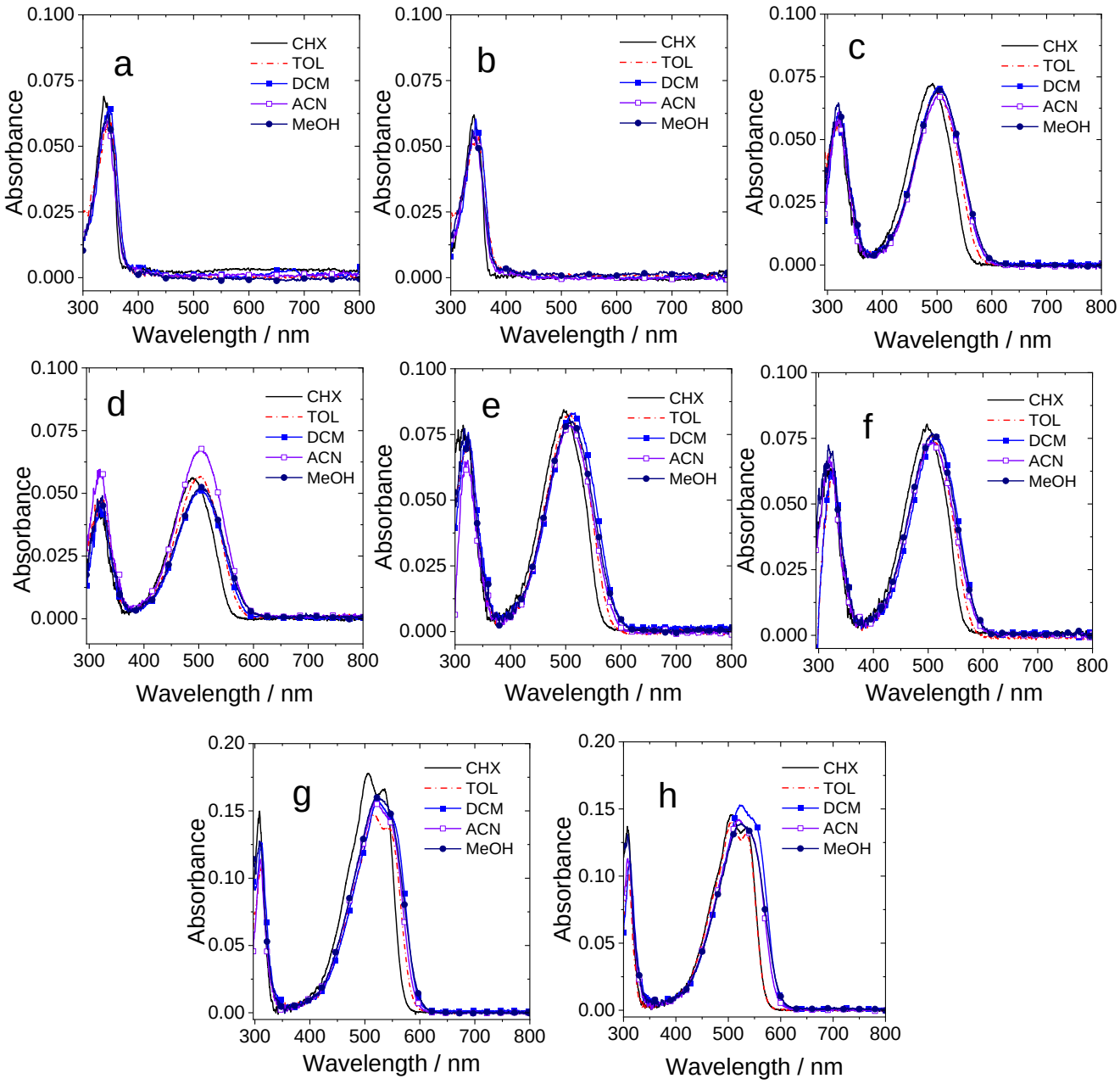

Figure S13. UV–vis absorption spectra of (a) **AQ-1,5-Cl2**; (b) **AQ-1,8-Cl2**; (c) **AQ-NH-OH-5-Cl**; (d) **AQ-NH-OH-8-Cl**; (e) **AQ-NH-5-Cl**; (f) **AQ-NH-8-Cl**; (g) **AQ-1,5-NH** and (h) **AQ-1,8-NH** in different solvents. c = 1.0 × 10^{-5} M, 20 °C.

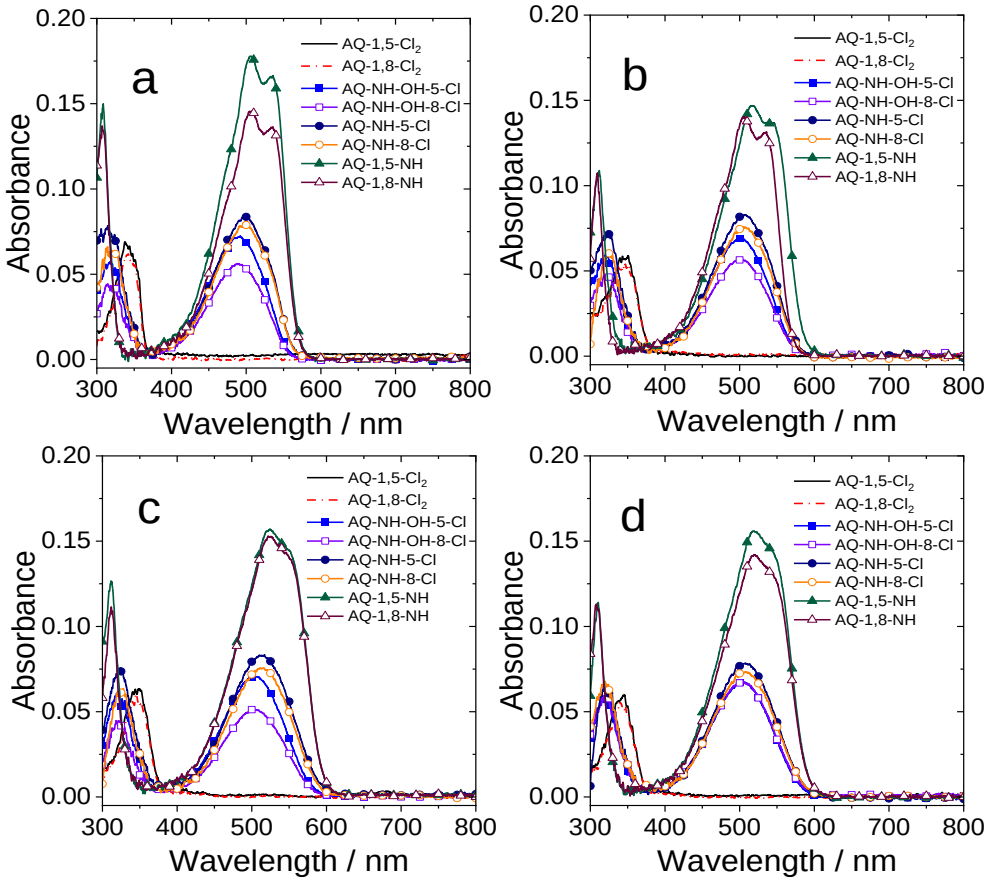

Figure S14. UV–vis absorption spectra of **compounds** in (a) cyclohexane (CHX); (b) toluene (TOL); (c) dichloromethane (DCM); (d) acetonitrile (ACN). $c = 1.0 \times 10^{-5}$ M, 20 °C.

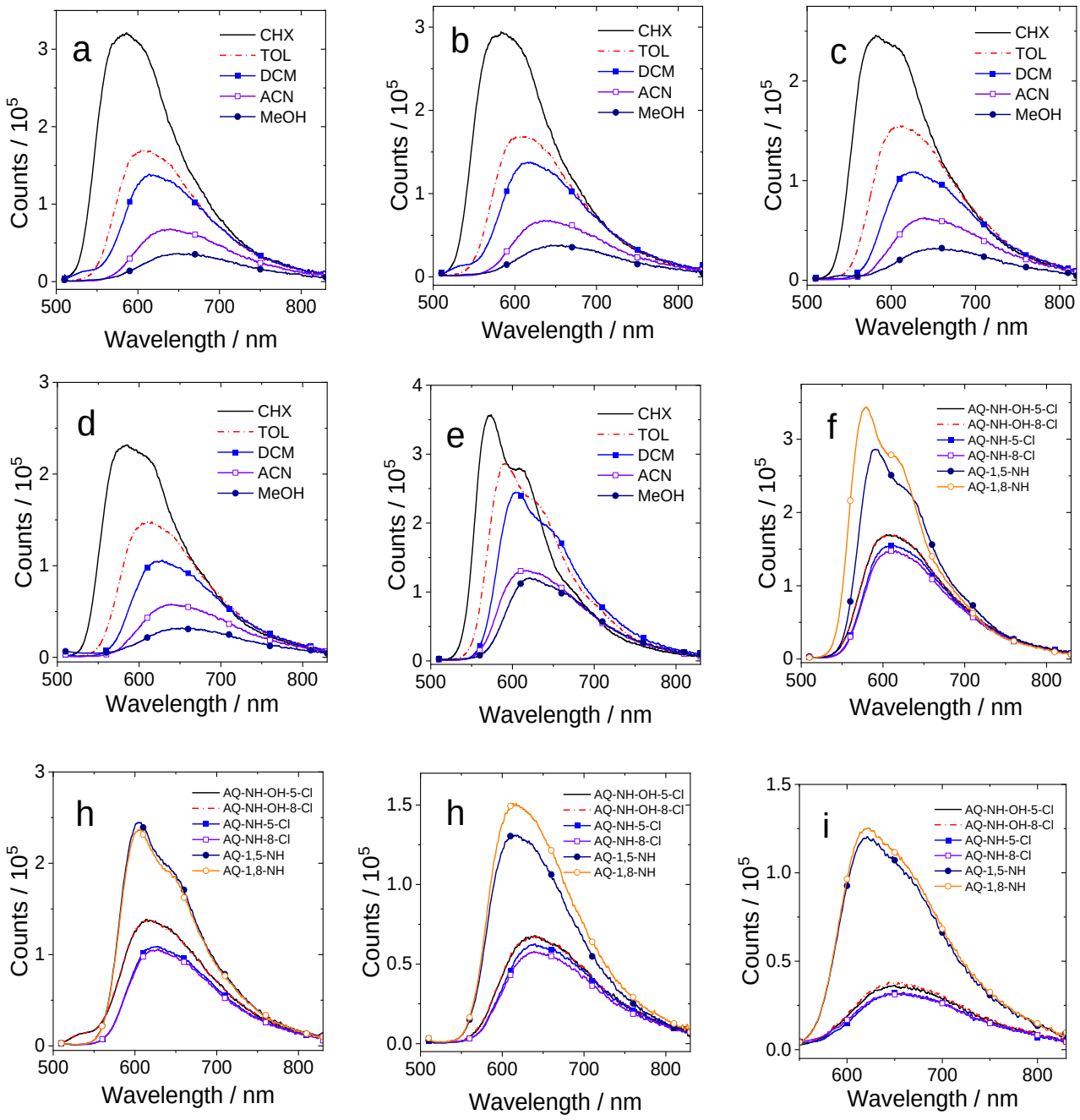

Figure S15. Fluorescence emission spectra of (a) **AQ-NH-OH-5-Cl**; (b) **AQ-NH-OH-8-Cl**; (c) **AQ-NH-5-Cl**; (d) **AQ-NH-8-Cl** and (e) **AQ-1,5-NH** in different solvents. Fluorescence emission spectra of compounds in (f) toluene (TOL); (g) dichloromethane (DCM); (h) acetonitrile (ACN); (i) Methanol (MeOH). Optically-matched solutions were used. A = 0.1, λ_{ex} = 500 nm, 20 °C.

3. Photobleaching and photopolymerization

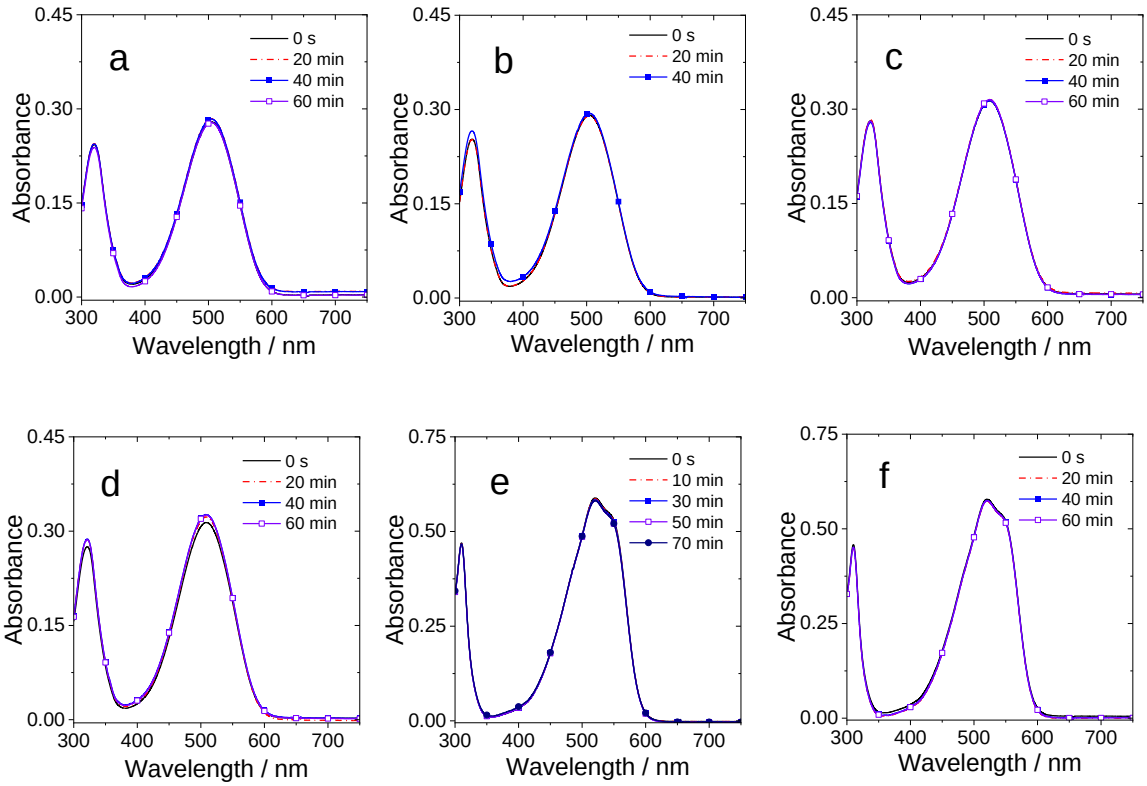

Figure S16. Steady state photolysis of (a) **AQ-NH-OH-5-Cl**; (b) **AQ-NH-OH-8-Cl**; (c) **AQ-NH-5-Cl**; (d) **AQ-NH-8-Cl**; (e) **AQ-1,5-NH** and (f) **AQ-1,8-NH** in deaerated acetonitrile upon the xenon lamp exposure; *c* [photosensitizer]=5.0 × 10^{-5} M. UV–vis spectra recorded at different irradiation times. unfiltered white light intensity = 30 mW cm^{-2}

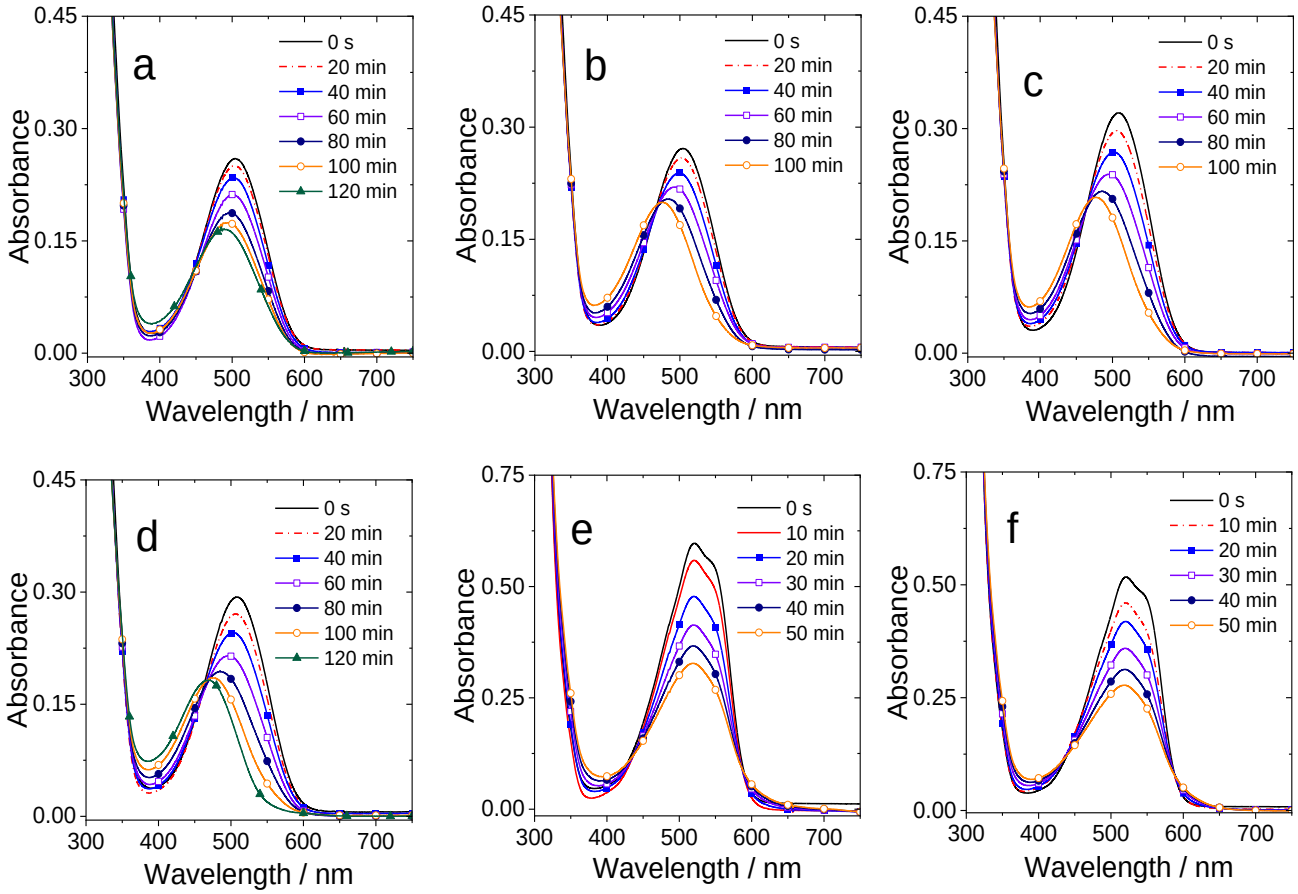

Figure S17. Steady state photolysis of (a) **AQ-NH-OH-5-Cl/DPI**; (b) **AQ-NH-OH-8-Cl/DPI**; (c) **AQ-NH-5-Cl/DPI**; (d) **AQ-NH-8-Cl/DPI**; (e) **AQ-1,5-NH/DPI** and (f) **AQ-1,8-NH/DPI** in deaerated acetonitrile upon the xenon lamp exposure; *c* [photosensitizer]=5.0 × 10^{-5} M , *c* [Iod] = 30 mM. Uv–vis spectra recorded at different irradiation times. unfiltered white light intensity = 30 mW cm^{-2}

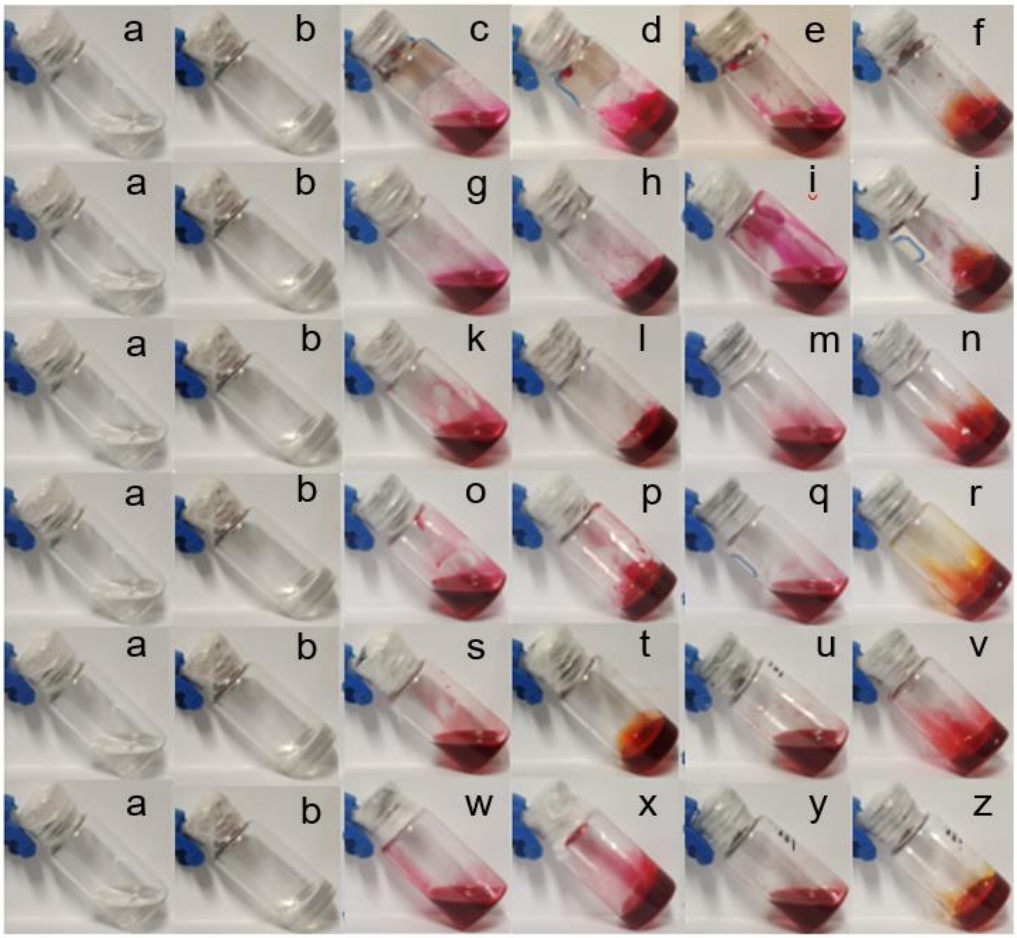

Figure S18. The photopolymerization of PETA under N_2 upon exposure to a 35 W Xenon lamp (unfiltered white light intensity = 200 mW cm^{-2}). In the presence of (a) **TEA**, (c) **AQ-1,5-NH**, (e) **AQ-1,5-NH/TEA**, (g) **AQ-1,8-NH**, (i) **AQ-1,8-NH/TEA**, (k) **AQ-NH-5-Cl,** (m) **AQ-NH-5-Cl/TEA,** (o) **AQ-NH-8-Cl,** (q) **AQ-NH-8-Cl/TEA,** (s) **AQ-NH-OH-5-Cl,** (u) **AQ-NH-OH-5-Cl/TEA,** (w) **AQ-NH-OH-8-Cl** and (y) **AQ-NH-OH-8-Cl/TEA.** The photopolymerization of PETA under N_2 upon exposure to a 35 W Xenon lamp (unfiltered white light intensity = 200 mW cm^{-2}). In the presence of (b) **TEA**, (d) **AQ-1,5-NH**, (f) **AQ-1,5-NH/TEA**, (h) **AQ-1,8-NH**, (j) **AQ-1,8-NH/TEA**, (l) **AQ-NH-5-Cl,** (n) **AQ-NH-5-Cl/TEA,** (p) **AQ-NH-8-Cl,** (r) **AQ-NH-8-Cl/TEA,** (t) **AQ-NH-OH-5-Cl,** (v) **AQ-NH-OH-5-Cl/TEA,** (x) **AQ-NH-OH-8-Cl** and (z) **AQ-NH-OH-8-Cl/TEA.** (photosensitizer: 0.3 wt%; TEA: 6.2 wt%)

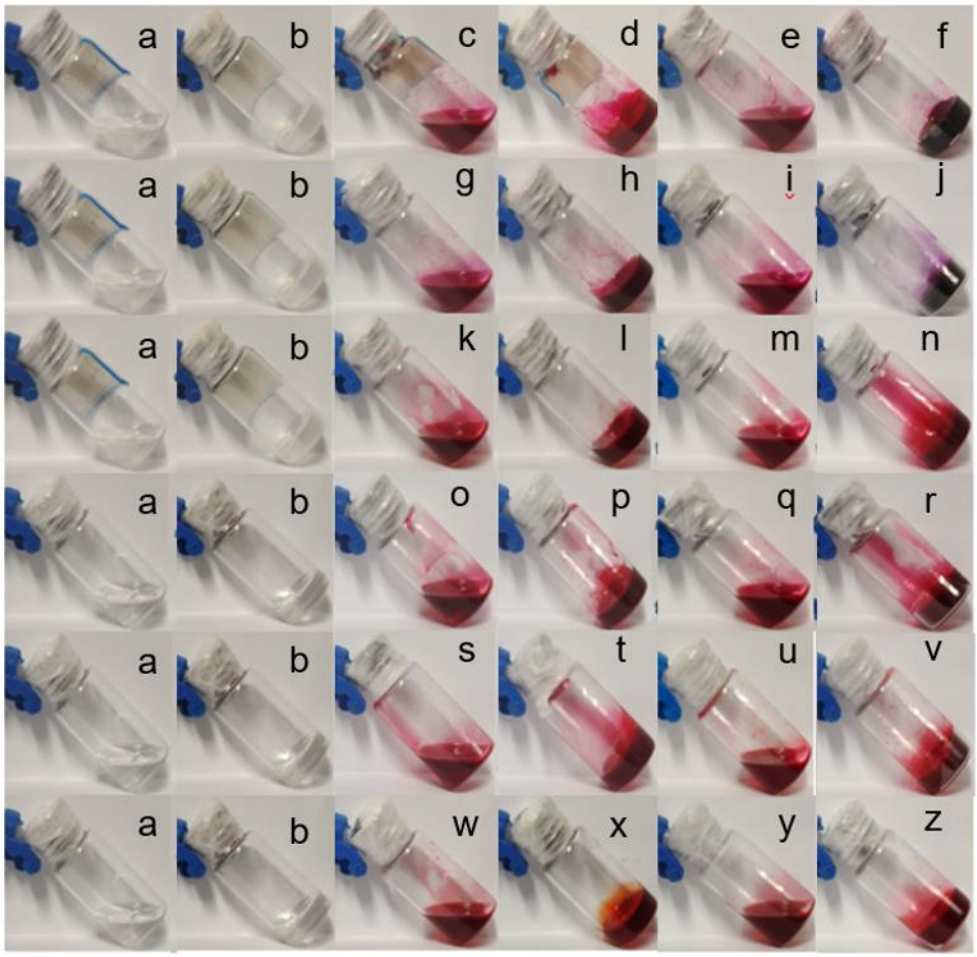

Figure S19. The photopolymerization of PETA under N_2 before a 35 W Xenon lamp irradiation (unfiltered white light intensity = 200 mW cm^{-2}). In the presence of (a) **DPI**, (c) **AQ-1,5-NH**, (e) **AQ-1,5-NH/DPI**, (g) **AQ-1,8-NH**, (i) **AQ-1,8-NH/DPI**, (k) **AQ-NH-5-Cl,** (m) **AQ-NH-5-Cl/DPI,** (o) **AQ-NH-8-Cl,** (q) **AQ-NH-8-Cl/DPI,** (s) **AQ-NH-OH-5-Cl,** (u) **AQ-NH-OH-5-Cl/DPI,** (w) **AQ-NH-OH-8-Cl** and (y) **AQ-NH-OH-8-Cl/DPI.** The photopolymerization of PETA under N_2 after a 35 W Xenon lamp irradiation (unfiltered white light intensity = 200 mW cm^{-2}). In the presence of (b) **DPI**, (d) **AQ-1,5-NH**, (f) **AQ-1,5-NH/DPI**, (h) **AQ-1,8-NH**, (j) **AQ-1,8-NH/DPI**, (l) **AQ-NH-5-Cl,** (n) **AQ-NH-5-Cl/DPI,** (p) **AQ-NH-8-Cl,** (r) **AQ-NH-8-Cl/DPI,** (t) **AQ-NH-OH-5-Cl,** (v) **AQ-NH-OH-5-Cl/DPI,** (x) **AQ-NH-OH-8-Cl** and (z) **AQ-NH-OH-8-Cl/DPI.** (photosensitizer: 0.3 wt%; DPI : 6.2 wt%).

Table S1. The photopolymerization of PETA obtained upon exposure to the Xeon lamp in the presence of anthraquinone derivatives based PISs[a]

PISs	The polymerization time of PETA/min
_[b]	_[c]
DPI	7
TEA	12
AQ-1,5-NH	8
AQ-1,5-NH/DPI	1
AQ-1,5-NH/TEA	5
AQ-1,8-NH	6
AQ-1,8-NH/DPI	0.6
AQ-1,8-NH/TEA	4
AQ-NH-5-Cl	10
AQ-NH-5-Cl/DPI	2.8
AQ-NH-5-Cl/TEA	7
AQ-NH-8-Cl	10
AQ-NH-8-Cl/DPI	3.5
AQ-NH-8-Cl/TEA	5
AQ-NH-OH-5-Cl	21
AQ-NH-OH-5-Cl/DPI	3.7
AQ-NH-OH-5-Cl/TEA	18
AQ-NH-OH-8-Cl	30
AQ-NH-OH-8-Cl/DPI	4.7
AQ-NH-OH-8-Cl/TEA	21

[a] The photopolymerization of PETA under N_2 in the presence of anthraquinone derivatives based PISs (photosensitizer: 0.3 wt%; DPI or TEA: 6.2 wt%) obtained upon exposure to the Xeon lamp, unfiltered white light intensity = 200 mW cm^{-2}. [b] In the absence of photosensitizer or coinitiator. [c] Can´t polymerization.

4. DFT computation

Table S2. Electronic Excitation Energies (eV) and Corresponding Oscillator Strengths (f), Main Configurations, and CI Coefficients of the Low-Lying Electronic Excited States of AQ-1,5-NH in gas phase were Presented. All Parameters were Calculated by B3LYP/6-31G(d). Base on the optimized ground state geometry.

	State	Energy[a]	f [b]	CI[c]	Composition[d]
AQ-1,5-NH	S_1	2.53 eV/489 nm	0.24	0.70	H→L
	S_7	4.25 eV/292 nm	0.18	0.69	H-1→ L+1
	S_8	4.47 eV/277 nm	0.08	0.66	H-5→L
	T_1	1.86 eV/666 nm	0.00	0.70	H→L
	T_2	1.87 eV/664 nm	0.00	0.70	H-1→L
	T_3	2.71 eV/458 nm	0.00	0.69	H-2→L
	T_4	2.91 eV/426 nm	0.00	0.55	H-5→L
	T_5	2.94 eV/421 nm	0.00	0.57	H-3→L

[a] Only the selected low lying excited states are presented. [b] Oscillator strengths. [c] CI coefficients are in absolute values. [d] Only the main configurations are presented.

Table S3. Electronic Excitation Energies (eV) and Corresponding Oscillator Strengths (f), Main Configurations, and CI Coefficients of the Low-Lying Electronic Excited States of AQ-1,8-NH in gas phase were Presented. All Parameters were Calculated by B3LYP/6-31G(d). Base on the optimized ground state geometry.

	State	Energy[a]	f [b]	CI[c]	Composition[d]
AQ-1,8-NH	S_1	2.40 eV/517 nm	0.21	0.70	H→L
	S_6	4.10 eV/303 nm	0.10	0.67	H→L+1
	S_7	4.33 eV/286 nm	0.06	0.66	H-1→L+1
	T_1	1.80 eV/691 nm	0.00 [g]	0.70	H→L
	T_2	1.93 eV/643 nm	0.00[g]	0.69	H-1→L
	T_3	2.56 eV/485 nm	0.00 [g]	0.67	H-2→L
	T_4	2.91 eV/425 nm	0.00[g]	0.54	H-3→L
	T_5	2.94 eV/421 nm	0.00 [g]	0.55	H-5→L

[a] Only the selected low lying excited states are presented. [b] Oscillator strengths. [c] CI coefficients are in absolute values. [d] Only the main configurations are presented.

Table S4. Electronic Excitation Energies (eV) and Corresponding Oscillator Strengths (f), Main Configurations, and CI Coefficients of the Low-Lying Electronic Excited States of AQ-NH-5-Cl in gas phase were Presented. All Parameters were Calculated by B3LYP/6-31G(d). Base on the optimized ground state geometry.

	State	Energy[a]	f [b]	CI[c]	Composition[d]
AQ-NH-5-Cl	S_1	2.56 eV/484 nm	0.13	0.70	H→L
	S_4	3.63 eV/341 nm	0.05	0.68	H-2→L
	S_6	3.86 eV/321 nm	0.06	0.53	H→L+1
	T_1	1.80 eV/687 nm	0.00 [g]	0.70	H→L
	T_2	2.38 eV/520 nm	0.00[g]	0.67	H-1→L
	T_3	2.84 eV/437 nm	0.00 [g]	0.39	H-3→L
	T_4	2.92 eV/425 nm	0.00[g]	0.67	H-4→L
	T_5	3.03 eV/409 nm	0.00 [g]	0.46	H-2→L

[a] Only the selected low lying excited states are presented. [b] Oscillator strengths. [c] CI coefficients are in absolute values. [d] Only the main configurations are presented.

Table S5. Electronic Excitation Energies (eV) and Corresponding Oscillator Strengths (f), Main Configurations, and CI Coefficients of the Low-Lying Electronic Excited States of AQ-NH-8-Cl in gas phase were Presented. All Parameters were Calculated by B3LYP/6-31G(d). Base on the optimized ground state geometry.

	State	Energy[a]	f [b]	CI[c]	Composition[d]
AQ-NH-8-Cl	S_1	2.52 eV/492 nm	0.12	0.70	H→L
	S_4	3.64 eV/341 nm	0.04	0.67	H-2→L
	S_6	3.84 eV/323 nm	0.05	0.50	H-4→L
	T_1	1.77 eV/700 nm	0.00	0.70	H→L
	T_2	2.49 eV/497 nm	0.00	0.66	H-1→L
	T_3	2.77 eV/448 nm	0.00	0.64	H-3→L
	T_4	2.81 eV/441 nm	0.00	0.35	H-4→L
	T_5	2.99 eV/414 nm	0.00	0.41	H-2→L

[a] Only the selected low lying excited states are presented. [b] Oscillator strengths. [c] CI coefficients are in absolute values. [d] Only the main configurations are presented.

Table S6. Electronic Excitation Energies (eV) and Corresponding Oscillator Strengths (f), Main Configurations, and CI Coefficients of the Low-Lying Electronic Excited States of AQ-NH-OH-5-Cl in gas phase were Presented. All Parameters were Calculated by B3LYP/6-31G(d). Base on the optimized ground state geometry.

	State	Energy[a]	f [b]	CI[c]	Composition[d]
AQ-NH-OH-5-Cl	S_1	2.56 eV/485 nm	0.13	0.70	H→L
	S_4	3.63 eV/341 nm	0.05	0.68	H-2→L
	S_6	3.85 eV/322 nm	0.06	0.53	H→L+1
	T_1	1.80 eV/689 nm	0.00	0.70	H→L
	T_2	2.38 eV/521 nm	0.00	0.67	H-1→L
	T_3	2.84 eV/437 nm	0.00	0.41	H-3→L
	T_4	2.93 eV/423 nm	0.00	0.66	H-4→L
	T_5	3.03 eV/409 nm	0.00	0.45	H-2→L

[a] Only the selected low lying excited states are presented. [b] Oscillator strengths. [c] CI coefficients are in absolute values. [d] Only the main configurations are presented.

Table S7. Electronic Excitation Energies (eV) and Corresponding Oscillator Strengths (f), Main Configurations, and CI Coefficients of the Low-Lying Electronic Excited States of AQ-NH-OH-8-Cl in gas phase are Presented. All Parameters were Calculated by B3LYP/6-31G(d). Base on the optimized ground state geometry.

	State	Energy[a]	f [b]	CI[c]	Composition[d]
AQ-NH-OH-8-Cl	S_1	2.52 eV/493 nm	0.12	0.70	H→L
	S_4	3.64 eV/340 nm	0.04	0.66	H-2→L
	S_6	3.83 eV/324 nm	0.06	0.51	H-4→L
	T_1	1.76 eV/703 nm	0.00	0.70	H→L
	T_2	2.50 eV/496 nm	0.00	0.66	H-1→L
	T_3	2.77 eV/447 nm	0.00	0.64	H-3→L
	T_4	2.81 eV/442 nm	0.00	0.36	H-4→L
	T_5	2.99 eV/414 nm	0.00	0.41	H-2→L

[a] Only the selected low lying excited states are presented. [b] Oscillator strengths. [c] CI coefficients are in absolute values. [d] Only the main configurations are presented.

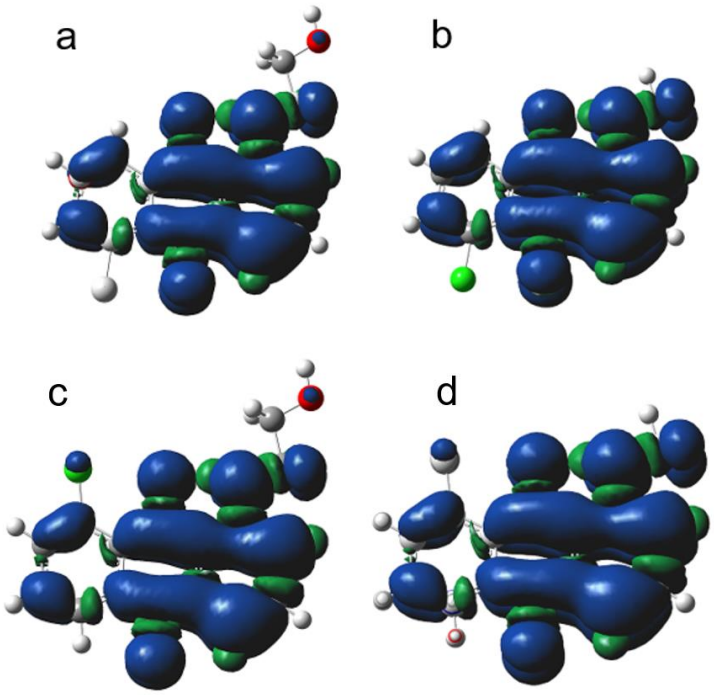

Figure S20. Electron spin density surfaces of the triplet state of (a) **AQ-NH-OH-5-Cl,** (b) **AQ-NH-5-Cl,** (c) **AQ-NH-OH-8-Cl** and (d) **AQ-NH-8-Cl** calculated by DFT (B3LYP/6-31G (d)) in vacuum with Gaussian 09**.** isovalue = 0.0004.